J Low Temp Phys (2012) 168:69–83
DOI 10.1007/s10909-012-0610-y

The Interplay Among Electrical, Magnetic, and Structural Properties in the Non-superconducting $Ru(Sr_{2-x}Ba_x)GdCu_2O_{8\pm z}$ System

M. Abatal · V. García-Vázquez · E. Chavira · G. González · A. Tejeda

Received: 14 September 2011 / Accepted: 27 February 2012 / Published online: 9 March 2012
© Springer Science+Business Media, LLC 2012

Abstract The electrical, magnetic, and structural properties of the non-superconducting $RuSr_2GdCu_2O_{8\pm z}$ system were studied through Ba substitution on the Sr sites. Samples of the non-superconducting $Ru(Sr_{2-x}Ba_x)GdCu_2O_{8\pm z}$ system, with $x = 0$, 0.05, 0.10, 0.15, 0.20, 0.25 and 0.50 were synthesized through the solid-state reaction method at ambient pressure, in air, at temperatures between 980 °C and 1025 °C. X-ray diffraction data show that substitution of Sr by Ba takes place iso-structurally into a tetragonal structure (space group $P4/mmm$, No. 123) with a solubility up to $x = 0.25$. Rietlveld-refinement analysis indicates that the cell volume monotonically increases with barium content, while both Cu–O(1) and [1–Ru–O(1)] bond lengths, as well as the Cu–O(2)–Cu bond angles, all increase with increasing x with a maximum peak around $x = 0.15$, and then all decrease for larger values of the barium content x, resulting into bell-type curves. The electrical resistance for the samples with $0 \leq x \leq 0.25$ annealed in flowing oxygen at 960 °C for 2 h shows a semiconducting behavior. DC-magnetization measurements indicate that all samples exhibit ferromagnetic ordering with a magnetic transition temperature T^{Curie} between 131 K and 141 K. Both the normalized resistance values (at a fixed temperature) and T^{Curie} show each a similar bell-type dependence on x, a result that seems to be similar to that found for the bond lengths and angles. These five bell-type dependences on x

M. Abatal (✉)
Facultad de Ingeniería, Universidad Autónoma del Carmen, C.P. 24180, Ciudad del Carmen, Campeche, México
e-mail: mabatal@pampano.unacar.mx

V. García-Vázquez
Instituto de Física LRT, Benemérita Universidad Autónoma de Puebla, A.P. J-48, Puebla, Pue, C.P. 72570, México

E. Chavira · G. González · A. Tejeda
Instituto de Investigaciones de Materiales, Universidad Nacional Autónoma de México, AP 70-360, 04510, México D.F., México

suggest that a strong interplay among electrical, magnetic and structural properties are taken place in the non-superconducting $Ru(Sr_{2-x}Ba_x)GdCu_2O_{8\pm z}$ system.

Keywords Rutheno-cuprates · XRD · Magnetic properties · Electrical properties

1 Introduction

The discovery of the hybrid rutheno-cuprate $RuSr_2GdCu_2O_8$ (Ru-1212) compound [1, 2] has been the subject of intense research due to the extraordinary coexistence of high-T_C superconductivity and long-range magnetic order [3, 4]. The Ru-1212 compound becomes superconducting at T_C values well below the magnetic transition T^{Curie}. Its crystal structure [5, 6] is derived from the $YBa_2Cu_3O_7$ (YBCO) compound, where Y and Ba are completely replaced by Gd and Sr, respectively, and the Cu–O chains in the charge reservoir block are replaced by RuO_2 planes [1, 7, 8]. The superconducting charge carriers originate from the conducting CuO_2 double layers, while the magnetic order sets in the RuO_2 layers, which also act as a charge reservoir for the conducting CuO_2 planes. The onset superconducting transition temperature, T_C (onset), and the temperature at which this material reaches zero resistance, T_C (zero), strongly depend on the details of sample preparation [8–14], where long annealing in flowing oxygen seems to be a necessary requirement for obtaining the superconducting phase [15].

Despite the intensive research on this material, various unanswered questions, however, still remain. The highly underdoped nature of $RuSr_2GdCu_2O_8$ compound, the mixed Ru valence state, and whether the superconducting and magnetic phases originate from a same crystallographic structure, are few of the aspects that are not well understood yet. Also important, is to clarify why a same stoichiometric and apparently iso-structural Ru-1212 compound produce both superconducting and non-superconducting samples. Some other but not less important concerns are exposed in the review articles given by Casini et al. [16], Klamut [17], Nachtrab et al. [18], Ovchinnikov [19], the book chapters given in Ref. [20] by Awana et al. (Chap. 3), Felner et al. (Chap. 2), and Lorentz et al. (Chap. 1), and the book chapters given in Ref. [21] by Braun et al. (Chap. 10), Chu et al. (Chap. 8), Masini et al. (Chap. 15), and Mclaughing et al. (Chap. 11).

In order to elucidate the interplay between superconductivity (SC) and ferromagnetism (FM) in the Ru-1212 compound, several substitutions in the Ru, Sr, Gd, and Cu sites have been carried out in the past few years. The substitution in the Sr sites of the Ru-1212 system, for example, by other cations from the alkaline earth group, such as Ba^{2+}, allows the study of the effects that the variations in the cell-parameters and the bond distances and angles have on the physical properties of the rutheno-cuprate compounds, particularly on the electrical and magnetic properties.

Yang et al. [22] have studied the superconducting properties of $RuSr_{2-x}Ba_x$-$GdCu_2O_8$ ($0 \leq x \leq 0.1$) and have found that the superconducting transition temperature is enhanced by Ba substitution on the Sr sites. They report that the superconducting transition temperature T_C depends on Ba content following a bell-type curve: first, T_C raises up to 35 K (zero) and 62 K (onset) for $x = 0.07$, from 16 K (zero)

and 45 K (onset) for $x = 0$; then, T_C decreases with x for $x > 0.07$, but with values larger than the T_C value obtained for $x = 0$. In other words, for $x \neq 0$, T_C is always larger than the value obtained for the undoped sample. They also report that the solid solution range is $0 \leq x \leq 0.1$, as determined by X-ray powder diffraction patterns. A detailed structural analysis of their samples show that in the region $x \leq 0.07$ (the raising size in their bell-type curve T_C vs. Ba content), with increasing x, the apical Cu–O(1) bond lengths stretch, while the Ru–O(1) bond lengths contract. The authors speculate that these two effects may be the main cause for the enhancement in T_C on this side of the bell-type curve.

Another report on Ba substitution on the Sr sites in the Ru-1212 system is given by Hur et al. [23]. They studied the interplay between magnetic coupling and superconductivity in $RuSr_2GdCu_2O_8$ compound by controlling the interlayer distance between the RuO_2 and CuO_2 layers via Ba substitutions on the Sr site. Although in their study the Ba content was not varied, they instead compared $RuSr_{1.9}A_{0.1}GdCu_2O_8$ with A = Ca, Sr, and Ba to examine the effect that the alkaline earth metal substitution has on the superconducting and electrical transport properties. They found that the superconductivity transition temperature is decreased in $RuSr_{1.9}Ba_{0.1}GdCu_2O_8$, from 31.8 K for the "pristine" compound (A = Sr) to 14.5 K for the Ba-substituted derivative, that is, a near 50 % reduction. With the aid of micro-Raman analysis, the depression in T_C upon the Ba substitution was explained later [24] in terms of the weakening that the internal charge transfer has between the RuO_2 and CuO_2 planes in the rutheno-cuprate. The result found by Hur et al. [23] seems to contradict the 50 % enhancement in T_C found for the $x = 0.10$ sample reported in the work given by Yang et al. [22].

Anyway, in both works on Ba substitution [22, 23], the starting, undoped composition ($x = 0$) was a superconducting $RuSrGdCu_2O_8$ compound. Results on equivalent substitutions deliberately performed on non-superconducting $RuSrGdCu_2O_8$ samples, however, were not given at all in both reports. Therefore, it seems necessary to investigate how properties, particularly the solid solution range, the lattice parameters, the bond distances and angles, and their correlation with the electrical and magnetic properties, would be affected if the starting, undoped samples were non-superconducting. As it is well known, nominally stoichiometric $RuSr_2GdCu_2O_8$ has also been reported as non-superconducting [25–27]. Non-superconducting $RuSr_2GdCu_2O_8$ samples seem to be produced by altering the synthesis conditions [25, 26] during sample preparation. Although the $RuSr_2GdCu_2O_8$ system is attractive due to its superconducting properties, particularly because they extraordinary coexist with magnetic ordering, significant results have also been obtained from studies deliberately performed on non-superconducting $RuSr_2GdCu_2O_8$ samples [28–34]. Matsubara et al. [28], for example, have investigated the magnetic and magneto-transport properties of a non-superconducting $RuSr_2GdCu_2O_8$ compound synthesized by a solid-state reaction method. In their work, a magnetic ordering of the Ru sublattice and an antiferromagnetic ordering of the Gd sublattice were individually observed at 148 K and 2.8 K, respectively, in non-superconducting $RuSr_2GdCu_2O_8$ samples. By analyzing the oxygen content and the tetragonal lattice parameters, they have concluded that the valence state of Ru is pentavalent in non-superconducting Ru-1212. Non-superconducting Ru-1212 samples have also been

used to measure their temperature-dependent specific heat C/T. Specific heat measurements are commonly used to investigate the bulk character of superconductivity in Ru-1212 [29–31], which manifests as a jump in the specific heat close to T_C. In the work given by Tallon et al. [29], however, the specific heat in a non-superconducting sample (produced by Zn substitution) was measured as a mean to "back off" the phonon contribution to the specific heat in regular superconducting samples. As a different example, Chen et al. [29] measured the heat capacity directly in an undoped, non-superconducting $RuSr_2GdCu_2O_8$ sample that contained small amounts of impurity phase Sr_2GdCuO_6 (Sr-2116) as a mean to rule out the suggestions proposed by Chu et al. [32] who argued that the anomalies observed in the heat capacity in superconducting $RuSr_2GdCu_2O_8$ samples [29] might as well be due to such an antiferromagnetic impurity phase. In their undoped, non-superconducting Ru-1212 reference sample, no anomaly was found in the specific heat data in the temperature range between 20 K and 50 K [29]. In contrast, a jump in the specific heat was found in related superconducting Ru-1212 samples containing the same amount of the impurity phase Sr-2116 [29], suggesting, therefore, that the specific heat jump arises from the superconducting transition. Non-superconducting Ru-1212 samples have also been used to measure the temperature dependence of the longitudinal and shear sound speed velocity and the ultrasonic attenuation to determine the elastic moduli and Debye temperature [33]. The Non-superconducting Ru-1212 system in the form of thin films has also been studied. $RuSr_2GdCu_2O_8$ thin films grown on (100) $SrTiO_3$ substrates have been prepared by Lebedev et al. [34] to investigate the structure of Ru-1212 on a local scale. Raman spectroscopy performed on superconducting as well as non-superconducting $RuSr_2GdCu_2O_8$ thin films prepared under comparable growth conditions [34] shows that there is no difference in peak position, peak broadness, or relative intensities in the Raman spectra.

Substitutions studies deliberately performed on non-superconducting samples, and the subsequent comparison with the investigations performed on the superconducting counterpart, may bring clues in the understanding of the extraordinary coexistence of magnetic order and superconductivity in the rutheno-cuprates. The non-superconducting phase not only is easier to reproduce, but also has the advantage that it does not manifest the coexistence of superconductivity and magnetic order. This permits to "remove" the superconducting aspect of the compound. In this paper, we investigate the interplay among electrical, magnetic, and structural properties of the non-superconducting $RuSr_2GdCu_2O_{8\pm z}$ system through substitution of Sr^{2+} by Ba^{2+} ions. The limit of solubility of $RuSr_{2-x}Ba_xGdCu_2O_8$ system is investigated, with x from 0 to $x = 0.50$ prepared by the solid-state reaction method at ambient pressure, in air. The purpose of our study is to offer complementary data by deliberately studying the non-superconducting counterpart of the Ru-1212 system.

2 Experimental Procedures

2.1 Synthesis

Samples with $x = 0, 0.05, 0.10, 0.15, 0.20, 0.25$, and 0.50 of the $RuSr_{2-x}Ba_x$-$GdCu_2O_8$ system were synthesized through a solid-state reaction technique at ambient pressure from stoichiometric amounts of RuO_2 (99.9 % STREM), Gd_2O_3

(99.99 %, STREM), CuO (99.99 %, ALDRICH), $BaCO_3$ (99.5 %, ALDRICH), and $SrCO_3$ (99.5 %, CERAC) compounds. Prior to weighing, $SrCO_3$ and $BaCO_3$ compounds were preheated for 10–20 min at 120 °C for dehydratation. A stoichiometric mixture for each desired composition was ground in an agate mortar in air. The reactions were carried out, also in air, in high alumina crucibles inside an electric furnace (±4 °C) operating at temperatures between 980 °C and 1025 °C for 24–72 h, with intermediate grindings of the samples. It is important to remark that for each composition in $RuSr_{2-x}Ba_xGdCu_2O_8$, different temperature ranges were used (see below). For $x = 0$, $T = 980$–1000 °C was utilized; for $0.05 \leq x \leq 0.15$, $T = 1000$–1015 °C; and for $0.20 \leq x \leq 0.50$, $T = 1000$–1025 °C. Following the treatment in air, X-ray data revealed that samples with $0.0 \leq x \leq 0.25$ presented a small $RuSrO_3$ impurity. Such an impurity, once formed, seems to be quite stable although difficult to remove during the reaction at higher temperatures [1, 2, 8]. The materials, therefore, were ground again and annealed in flowing argon at 960 °C after calcinations in air. With this particular procedure, the formation of such $RuSrO_3$ impurity was reduced only on the samples with $0.05 \leq x \leq 0.25$. The resulting powders were pressed into pellets and annealed at 960 °C for only 2 h in flowing oxygen and then slowly cooled down to room temperature. We have chosen this lower temperature value because in previous studies where Thermogravimetry analysis was performed, we had observed that Ru-1212 compound begins to lose oxygen once $T = 960$ °C is reached [35]. In addition, the annealing time was reduced to 2 h to assure that samples not only have a semiconducting phase, but also be non-superconducting, the purpose of our study.

2.2 Reaction Temperatures

In order to obtain the precise temperature interval at which the reaction must be accomplished for the formation of the Ru-1212 phase in each composition, differential thermal analysis (DTA) in air was carried out on the samples. DTA experiments were performed using a Modulated DSC 9210, TA instruments. Samples were placed in platinum crucible and heated from ambient temperature to 1200 °C at a heating rate of 10 °C/min in air.

2.3 Characterization Methods

XRD patterns were obtained on a Siemens D5000 diffractometer with Cu $K\alpha_1$ radiation. Diffraction patterns were collected at room temperature over the 2Θ range of 10–70° with a step size of 0.02° and a time-per-step constant of 10 secs. Refinement of the crystal structures was carried out using the Rietveld method with the aid of the *FullProf program* [36]. High-precision electrical resistance measurements, as a function of temperature, were performed in a closed cycle refrigerator instrumented with low-level measurement equipment. The four-probe technique, in combination with a commutation method in a constant-current mode, was utilized [37]. Copper wires (No. 38, 99.9985 % pure) were connected on the surface of the samples and were attached using commercial silver paint. Therefore, surface resistance, rather that bulk resistance, is reported here. Applied current used in all samples was 1.0 mA. In all experiments, resistance data were taken with increasing temperature, from 9 K to room

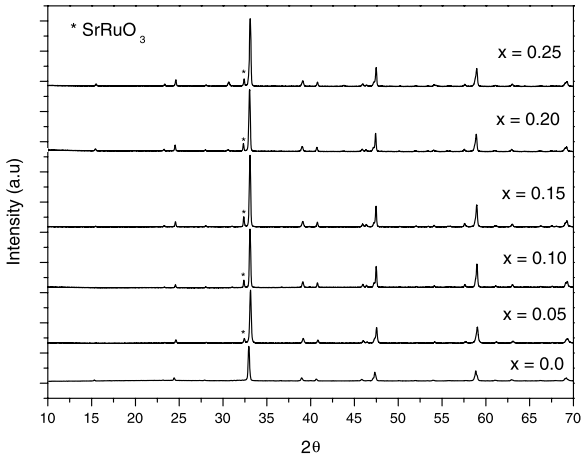

Fig. 1 XRD patterns of the $RuSr_{2-x}Ba_xGdCu_2O_8$ system

temperature. DC-magnetization measurements were performed in a superconducting quantum interference devise (SQUID) based magnetometer, in the temperature range of 4–250 K. The samples were pressed and wrapped with a very small piece of Teflon tape and then suspended into the stem.

3 Results and Discussions

DTA results show several endothermic transitions in the following temperature ranges: (1) $T = 655$–738 °C, which corresponds to the oxisals decomposition and the beginning of secondary reactions; (2) $T = 894$–985 °C, which can be attributed to the formation of the Ru-1212 phase and other different compounds; and (3) $T = 1217$–1350 °C, which is related to the fusion of the material. X-ray diffraction patterns of the $RuSr_{2-x}Ba_xGdCu_2O_8$ system are shown in Fig. 1. It can be seen here that for $x = 0$, the sample is single phase, whereas for samples with $x = 0.05, 0.10, 0.15, 0.20$ and 0.25, small additional intensities are observed. These additional reflections are attributed to the formation of the $SrRuO_3$ phase [1]. It is well known that the $SrRuO_3$ compound reveals magnetic order around 165 K [2]. However, we have found (see below) no appreciable anomalies in the magnetic or the electrical measurements around this temperature, indicating, therefore, that the amount of spurious phases is only marginal. All X-ray diffraction patterns, obtained at room temperature on the investigated samples, revealed the same primitive tetragonal structure of the undoped $RuSr_2GdCu_2O_8$ compound (Fig. 1). The Ba^{2+} substitution for the Sr^{2+} sites into a single Ru-1212 phase is successful only up to a 25 % of Ba. For the sample with $x = 0.50$, a mixture of $SrRuO_3$, Sr_2GdRuO_6, and Ru-1212 phases was detected.

The XRD patterns of all samples were Rietveld-fitted, taken into account the possibility that the Ba ion can also occupy the Sr ion sites. The presence of $SrRuO_3$ secondary phase was included using a space group (sp. gr.) $P4/mmm$ (No. 123). The Ru ions occupy the crystallographic $1b$ sites $(0, 0, 0.5)$; Gd ions, the $1c$ sites $(0.5, 0.5, 0)$; Sr and Ba ions, the Wyckoff position $2\,h(0.5, 0.5, z)$; Cu, the $2g$ position

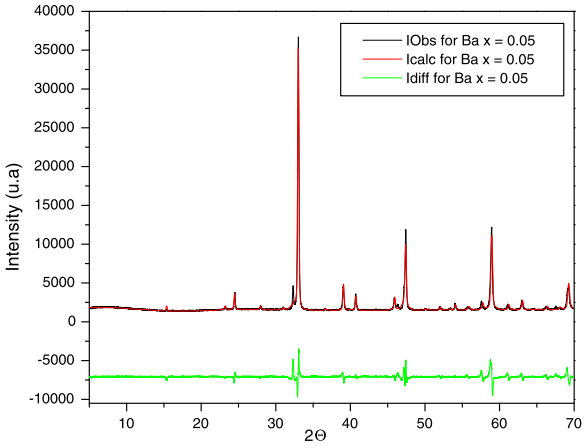

Fig. 2 Rietveld refinement of the XRD pattern for the $x = 0.05$ sample (*Color figure online*)

Table 1 Refined structural parameters of the $RuSr_{2-x}Ba_xGdCu_2O_8$ system (sp. gr. $P4/mmm$)

x	0	0.05	0.10	0.15	0.20	0.25
a (Å)	3.83047	3.83094	3.83204	3.83254	3.83289	3.83284
c (Å)	11.50848	11.51923	11.52070	11.52403	11.52723	11.53290
V (Å^3)	168.8582	169.0574	169.1761	169.2691	169.3471	169.3627
z (Sr)	0.323(9)	0.322(5)	0.327(2)	0.326(7)	0.321(3)	0.317(9)
z (Cu)	0.153(9)	0.150(3)	0.149(8)	0.149(9)	0.147(9)	0.146(4)
x (O1)	0.051(3)	0.051(0)	0.051(0)	0.051(0)	0.051(0)	0.051(0)
z (O1)	0.3134)	0.317(1)	0.320(9)	0.319(5)	0.315(2)	0.313(2)
z (O2)	0.087(0)	0.084(0)	0.088(5)	0.086(2)	0.084(6)	0.081(2)
x (O3)	0.122	0.122	0.122	0.122	0.122	0.122
N (Ba)	0	0.003125	0.00625	0.009375	0.0125	0.015625
R Bragg	6.80	8.95	9.07	9.38	9.20	9.94
RF	3.46	4.58	4.64	4.80	4.73	4.76

$(0, 0, z)$; and the oxygen ions, distributed among the 8 $s(x, 0, z)$, the 4 $o(x, 0.5, 0.5)$, and the 4 $i(0, 0.5, z)$ positions. The oxygen sites in the SrO, CuO_2, and RuO_2 planes are denoted by O(1), O(2) and O(3), respectively. N(Ba) represents the occupancy parameter for Ba ion in the Sr ion site.

Figure 2 shows the diffraction data and the final Rietveld-refinement for the sample with $x = 0.05$. The results of the refinement of the X-ray diffraction patterns for all samples are summarized in Table 1. From these results, we can confirm that the Ba ions indeed occupy the Sr ion sites. In addition, we can see that the structural parameter values of the undoped ($x = 0$) sample are in agreement with other published results [5, 6].

Figure 3 shows the variation of the lattice parameters and the unit-cell volume with the Ba ion content x. It can be seen here that the partial substitution of Ba^{2+} for Sr^{2+} is accompanied by an insignificant although monotonically increase in the

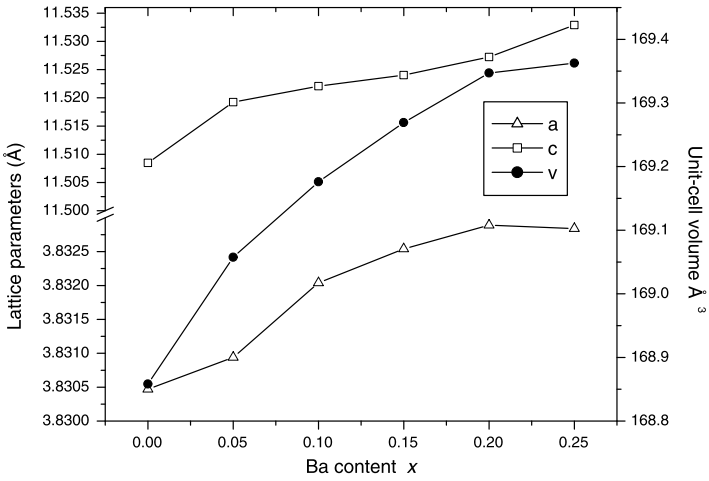

Fig. 3 Lattice parameters and unit-cell volume as a function of Ba content. The *symbols* represent the experimental data whereas the *lines* are introduced as guides to the eye

Table 2 Bond lengths and angles of the $RuSr_{2-x}Ba_xGdCu_2O_8$ system

x	0	0.05	0.10	0.15	0.20	0.25
Bond lengths (Å)						
Ru–O(1)	2.1568	2.1161	2.0891	2.0731	2.1391	2.1628
Ru–O(3)	1.9715	1.9717	1.9725	1.9723	1.9727	1.9727
Cu–O(1)	1.8452	1.9313	1.9643	1.9808	1.9383	1.9343
Cu–O(2)	2.0645	2.0619	2.0520	2.0420	2.0506	2.0585
Bond angles (degrees)						
Ru–O(3)–Ru	152.56	152.56	152.56	152.56	152.56	152.56
Cu–O(2)-Cu	136.08	136.56	138.12	139.43	138.37	137.31
Cu–O(1)–Ru	168.70	168.88	168.91	168.91	168.95	168.98

a-axis, while the c-axis shows a considerable and also monotonically increase with x. The net effect of both lattice parameters is an appreciable increase in the unit-cell volume when increasing x, a result that can be attributed to the fact that the Ba ion is larger than the Sr one (IR^{XII} $Ba^{2+} = 1.61$ Å and IR^{XII} $Sr^{2+} = 1.44$ Å) [38]. These results suggest, therefore, that Ba ions successfully substitute for Sr.

Table 2 shows the Rietveld-fitted bond lengths and angles of the $RuSr_{2-x}Ba_x$-$GdCu_2O_8$ system. The apical oxygen atoms O(1) of the CuO_5 square pyramid are closer to the Sr ion site and are, therefore, the most affected by the Ba ion substitution. The Rietveld-refinement results presented in this table also show a dependence of the Cu–O(1) bond lengths on the Ba content x. The Cu–O(1) bond lengths increase with increasing x, get a maximum value around $x = 0.15$, and then decrease again with x, following a bell-type curve. Another dependence on the Ba content is observed in the Ru–O(1) bond lengths, although an opposite behavior is found, that is, that

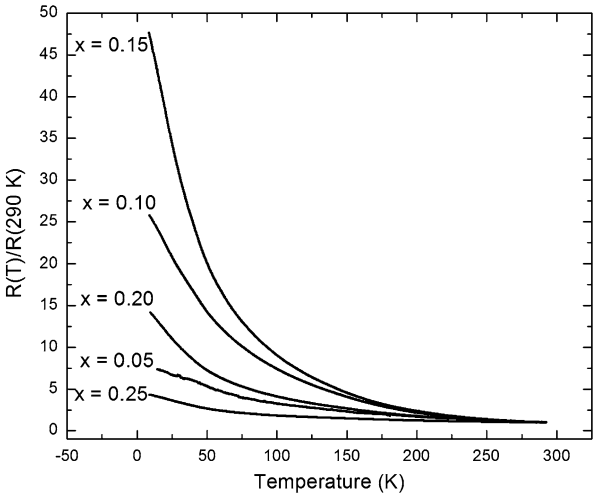

Fig. 4 Normalized resistance as a function of temperature of the $RuSr_{2-x}Ba_xGdCu_2O_8$ system

of an upside-down bell type curve centered again around $x = 0.15$. In contrast, it is observed that the Cu–O(2) and Ru–O(3) distances remain unchanged at the values of 2.06 and 1.97 Å, respectively.

For the characteristic angles in the structure, the following behaviors with increasing x are observed. (a) The bond angle Cu–O(1)–Ru, which is associated to the deviation of the apical oxygen O(1) along the plane perpendicular to the c-axis and whose value determines the distortion of the RuO_6 octahedra, (essential for the magnetic exchange interaction), shows no significant changes. (b) The bond angle Ru–O(3)–Ru, which is a measure of the rotation of the RuO_6 octahedra around the c-axis, remains extraordinarily constant. (c) The bond angle Cu–O(2)–Cu, which is a measure of the buckling of the CuO_2 layer, seems to have a dependence on the Ba content x: as x increases, the bond angle Cu–O(2)–Cu increases, reaches a maximum at $x = 0.15$, and then decreases again. Once again, a bell-type curve is found.

Figure 4 shows the normalized electrical resistance R as a function of temperature T from 9 K to room- temperature for the $RuSr_{2-x}Ba_xGdCu_2O_8$ samples with $x = 0.05, 0.10, 0.15, 0.20$ and 0.25. All samples show a same characteristic semiconducting behavior, *i.e.*, as temperature increases, resistance decreases. In all five samples tested, no superconductivity was found in the measured temperature interval; no semiconducting-to-metal transition was found either.

These results, together with the magnetic measurements discussed below, indicate, therefore, that the procedure for the sample preparation used in this study effectively produces $RuSr_{2-x}Ba_xGdCu_2O_8$ samples that are non-superconducting. Consequently, the above structural properties found for the lattice parameters, as well as the corresponding relationships observed for bond lengths and angles are, indeed, characteristic features of the non-superconducting nature that the $RuSr_{2-x}Ba_xGdCu_2O_8$ system is able to manifest.

Figure 5 shows the normalized resistance as a function of Ba content at several fixed temperatures.

In all these profiles, the same bell-type curve is obtained, that is, as Ba content increases, normalized resistance values increase, reach a maximum around the Ba

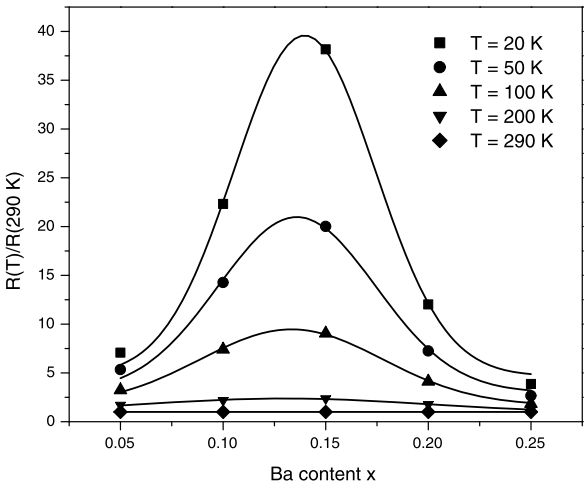

Fig. 5 Normalized resistance as a function of Ba content. The *lines* through the points are guides to the eye

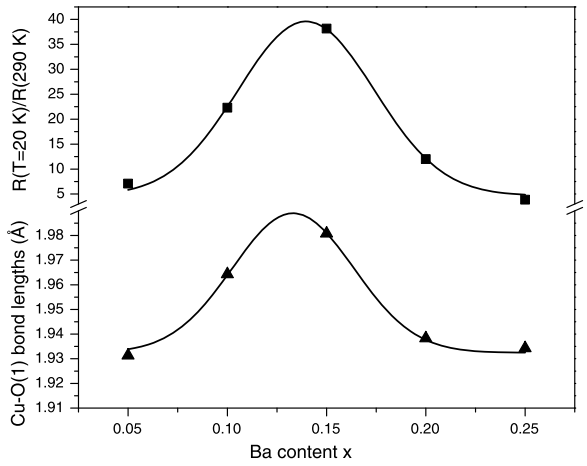

Fig. 6 Cu–O(1) bond distances and normalized resistance values versus Ba content. The *lines* are guides to the eye

content $x = 0.15$, and then decrease again. Similar behavior was observed at all temperatures measured, as it can be seen directly in Fig. 4; there, it is noted that there is not any line-crossing among the curves with different Ba content.

In order to explain the bell-type variation of the normalized resistance on the Ba content, two possibilities are proposed here: (1) that there is a change in the environment at the Sr site due to Ba doping, and (2) that there is a change in the electronic structure due to the modification of the Cu–O(1) and Ru–O(1) bond lengths. Rietveld refinement results showed in Table 2 confirm that the Cu atoms displace slowly to a lower position along the *c*-axis and, on the other hand, we note that both Cu–O(1) and Ru–O(1) bond lengths change with Ba content. Figure 6 compares the variations of Cu–O(1) bond distances (bottom) and one of the normalized resistance values (top) versus Ba content. It is noted that both curves, obtained from different characterization techniques performed on the same non-superconducting samples, share a same

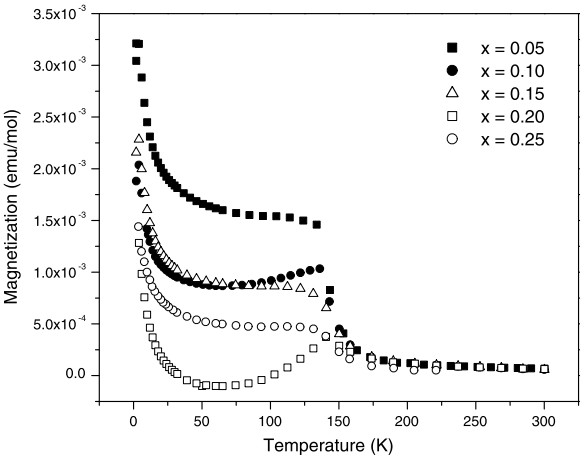

Fig. 7 DC-magnetization as function of temperature of the $RuSr_{2-x}Ba_xGdCu_2O_8$ system

bell-type behavior, confirming in this way our interpretation. Furthermore, as previously explained, a similar bell-type behavior also was found in the Cu–O(2)–Cu bond angle, which is a measure of the buckling of the CuO_2 layer.

The effect that the Ba content has on the Cu–O(1) bond distances of non-superconducting $RuSr_{2-x}Ba_xGdCu_2O_8$ samples (Fig. 6) seems to be similar, at least in shape, with the one reported by Yang et al. [22] for superconducting $RuSr_{2-x}Ba_xGdCu_2O_8$ samples. This similarity suggests that both superconducting and non-superconducting phases in Ru-1212 might share, apparently, the same crystal structure. For the electrical properties, however, the effects are opposite. Our bell-type curves for the normalized resistance (Fig. 5) appear to have the opposite effect found in the work given by Yang et al. (*ibid.*) on the superconducting counterpart. First, in the normal state, their samples are metallic (and not semiconducting as it is in our case). Second, they found that it is the perfect conductivity (and not the resistance as it is in our case) the one that is enhanced with Ba content, as quantified by the enhancement of the superconducting transition temperature T_C (Fig. 4 in Ref. [22]). These opposite results in the electrical properties, however, might not be contradictory but rather complementary to each other. Our results on non-superconducting Ru-1212 samples, however, seems to be more consistent with the works performed on superconducting $RuSr_{1.9}Ba_{0.1}GdCu_2O_8$ given by Hur et al. [23] and Kim et al. [24] who found that Ba has a detrimental effect on T_C, a result that seems to be more consistent with the increase of the normalized resistance found in our $x = 0.10$ non-superconducting sample. Taking into account that the hole density in the superconducting CuO_2 planes is provided by the charge transfer from the hole-reservoir RuO_2 layer, Kim et al. [24] have attributed the T_C depression in their superconducting $RuSr_{1.9}Ba_{0.1}GdCu_2O_8$ and $RuSr_{1.9}Ca_{0.1}GdCu_2O_8$ compositions to the depression of the internal charge transfer in the rutheno-cuprates.

Figure 7 shows the temperature dependence of the DC-magnetization measurements, $M(T)$, performed in an applied magnetic field $H = 10$ Oe. We observe that all samples show the characteristic ferromagnetic ordering transition curves at temperatures between 131 K and 141 K. Sample with $x = 0.20$, however, shows a negative diamagnetic signal in the DC magnetic susceptibility at temperatures between

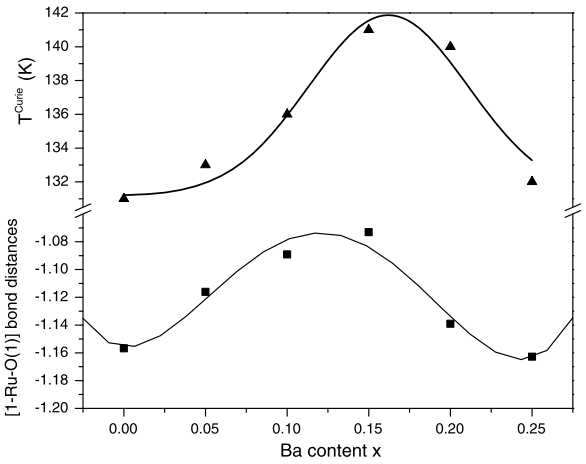

Fig. 8 [1–Ru–O(1)] bond distances and T^{Curie} values versus Ba content. The *lines* are guides to the eye

40 K and 100 K, approximately. For all samples, $M(T)$ curves show an increase in the magnetization due to the paramagnetic contribution of the Gd ions. The Gd sublattice remains in the paramagnetic state when the Ru sublattice is ordered ferromagnetically at $T \sim 130$ K.

An interesting result that can be observed from the Rietveld refinement X-ray data (Table 2) is that, as previously mentioned, there are no significant changes in the Ru–O(3)–Ru and Cu–O(1)–Ru bond angles for our non-superconducting $RuSr_{2-x}Ba_xGdCu_2O_8$ samples. The bond angles offer a measure of the canting of the Ru magnetic moment necessary to explain the appearance of ferromagnetism. Therefore, it seems that the magnetic order found in both superconducting [22] and non-superconducting $RuSr_{2-x}Ba_xGdCu_2O_8$ systems cannot be attributed to a change in these particular bond angles. Rather, it might occur because the substitution is carried out on the Sr sites, where both Sr^{2+} and Ba^{2+} ions present diamagnetic behavior.

In addition to the four bell-type dependences discussed so far (the normalized resistance, the Cu–O(1) bond distances, the Cu–O(2)–Cu bond angles, and the upside-down Ru–O(1) bond lengths), a fifth bell-type dependence on the Ba content was observed in this study. Figure 8 shows the ferromagnetic transition temperature T^{Curie} (top) extracted from the magnetic measurements (Fig. 7), and the relative distance that the Ru–O(1) bond length makes with respect to 1 Angs. (bottom). The subtraction to 1 Angstrom was done here with the purpose of turning over the upside-down bell-type curve found in the Ru–O(1) bond length, as previously mentioned. As can be seen in Fig. 8, the relative distance [1–Ru–O(1)], in Angs., increases with increasing Ba content with a maximum peak around $x = 0.15$, and then decreases for larger values of x, resulting into a broad peak. Similarly, T^{Curie} values show a broad peak centered around $x = 0.15$. Both curves show a bell-type dependence with x.

This interesting result indicates that the above mentioned magnetic behavior of the non-superconducting $RuSr_{2-x}Ba_xGdCu_2O_8$ system is indeed associated to a structural change induced by the Ba substitution, in spite of Sr^{2+} and Ba^{2+} ions present diamagnetic behavior. After all, the Ru ions that appear in the Ru–O(1) bond distances not only contribute to the layers of the charge reservoir, but also are responsible for the occurrence of the magnetic order in the Ru-1212 compound. Therefore, it

is expected that a Ba-induced modification in the Ru–O(1) distances be accompanied by a similar change in the magnetic properties, in this case, in the magnetic transition temperature.

Note, however, that this particular dependence of the ferromagnetic transition temperature on the Ba content found for the non-superconducting Ru-1212 contrasts with that reported by Yang et al. [22]. They found that the substitution of Ba^{2+} for Sr^{2+} ions in superconducting samples does not change the ferromagnetic transition temperature ($T_M = 136$ K). These opposite results obtained from the Ba substitution on the two phases that the Ru-1212 system is able to manifest in its electrical transport properties (superconducting and non-superconducting) seem to be complementary rather than contradictory. Our results, however, not only permit the observation of variations in the ferromagnetic temperature transition in the non-superconducting $RuSr_{2-x}Ba_xGdCu_2O_8$ system, but also offer a direct correlation with the changes in the Ru–O(1) bond-lengths. This brings the question whether the non-superconducting phase is responsible or not to enhance the observation of appreciable changes in the ferromagnetic transition temperature when the Sr ions are substituted by Ba ions. The five instances of bell-type curves found among the structural, electrical, and magnetic properties and the occurrence of their maximum values at nearly the same Ba content x (nearly $x = 15$) may bring clues to elucidate the extraordinary coexistence of superconductivity and magnetism found in the undoped $RuSr_2GdCu_2O_8$ system.

4 Conclusions

The interdependence among electrical, magnetic, and structural properties of the non-superconducting $RuSr_2GdCu_2O_{8\pm z}$ system was studied through substitution of Sr^{2+} by Ba^{2+} ions. Solid solutions from $x = 0$ up to $x = 0.25$ were obtained with $RuSr_{2-x}Ba_xGdCu_2O_8$ by the solid-state reaction method at ambient pressure. Rietveld-refinement results show that all samples are iso-structural with the undoped Ru-1212 compound, though cell volume does increase with barium content. Temperature-dependent resistance profiles show a semiconducting behavior in all samples, with no transition to a metal or a superconducting phase, confirming that the samples are indeed non-superconducting. Even so, normalized resistance values at a fixed, arbitrary temperature show a bell-type dependence on Ba content x, a behavior that seems to be the same for all temperatures tested, from room temperatures down to 9 K. A similar bell-type dependence on Ba content was found in the Cu–O(1) bond lengths obtained at room temperature. This study proves that it exists a relationship between the variation of Cu–O(1) bond lengths and the electrical properties in the non-superconducting Ru-1212 system. A similar conclusion was obtained in the superconducting counterpart [22]. However, in this work, we also found an additional bell-type dependence on the Ba content for the Cu–O(2)–Cu bond angles. Chemical substitution usually affects several parameters at once, and this study was not the exception since further bell-type dependences on the Ba content x were also found in both the Ru–O(1) bond lengths and the ferromagnetic transition temperatures. This last result contrasts with the superconducting counterpart [22], where not changes were observed in the ferromagnetic transition temperatures as the

Ba content was varied. Our results indicate, therefore, that the non-superconducting $RuSr_{2-x}Ba_xGdCu_2O_8$ system seems to be more sensitive to the substitution of Ba in the Sr sites, and the variations observed in the magnetic properties are associated to a structural change induced by the Ba substitution.

Acknowledgements The authors acknowledge financial support provided by CONACYT (Grant No. 80380), OCI UNAM-UNACAR, and VIEP-BUAP.

References

1. L. Bauernfeind, W. Widder, H.F. Braun, Physica C **254**, 151 (1995)
2. L. Bauernfeind, W. Widder, H.F. Braun, J. Low Temp. Phys. **105**, 1605 (1996)
3. J.L. Tallon, C. Bernhard, M. Bowden, P. Gilberd, T. Stoto, D. Pringle, IEEE Trans. Appl. Supercond. **9**, 1696 (1999)
4. C. Bernhard, J.L. Tallon, Ch. Niedermayer, Th. Blasius, A. Golnik, E. Brücher, R.K. Kremer, D.R. Noakes, C.E. Stronack, E.J. Asnaldo, Phys. Rev. B **59**, 14099 (1999)
5. A.C. McLaughlin, W. Zhou, J.P. Attfield, A.N. Fitch, J.L. Tallon, Phys. Rev. B **60**, 7512 (1999)
6. O. Chmaissem, J.D. Jorgensen, H. Shaked, P. Dollar, J.L. Tallon, Phys. Rev. B **61**, 6401 (2000)
7. L. Bauernfeind, W. Widder, H.F. Braun, in *High T_c Superconductors*, vol. 6, ed. by A. Barone, D. Fiorani, A. Tampieri (Gruppo Editoriale Faenza S.p.A., Faenza, 1995) p. 329
8. L. Bauernfeind. Ph.D. Thesis Universität Bayreuth, July 1998
9. P.W. Klamut, B. Dabrowski, S.M. Mini, M. Maxwell, S. Kolesnik, J. Mais, A. Shengelaya, R. Khasanov, I. Savic, H. Keller, T. Graber, J. Gebhardt, P.J. Vicarro, Y. Xiao, Physica C **364–365**, 313 (2001)
10. P.B. Lorenz, R.L. Meng, J. Cmaidalka, Y.S. Wang, J. Lenzi, Y.Y. Xue, C.W. Chu, Physica C **363**, 251 (2001)
11. C. Artini, M.M. Carnasciali, G.A. Costa, M. Ferretti, M.R. Cimberle, M. Putti, R. Masini, Physica C **377**, 431 (2002)
12. S. Chen, H.F. Braun, T.P. Papageorgiou, J. Alloys Compd. **351**, 7 (2003)
13. P.W. Klamut, B. Dabrowski, S.M. Mini, M. Maxwell, J. Mais, I. Felner, U. Asaf, F. Ritter, A. Shengelaya, R. Khasanov, I.M. Savic, H. Keller, A. Wisniewski, R. Puzniak, I.M. Fita, C. Sulkowski, M. Matusiak, Physica C **387**, 33 (2003)
14. H.F. Braun, in *Frontiers in Superconducting Materials*, ed. by A.V. Narlikar (Springer, Berlin, 2005), p. 365
15. A.C. McLaughlin, W. Zhou, J.P. Attfield, A.N. Fitch, J.L. Talon, Phys. Rev. B **60**, 7512 (1999)
16. E. Casini, M. Kempf, J. Krämer, H.F. Braun, J. Phys., Condens. Matter **21**, 254210 (2009)
17. P.W. Klamut, Supercond. Sci. Technol. **21**, 093001 (2008)
18. T. Nachtrab, Ch. Bernhard, C.T. Lin, D. Koelle, R. Kleiner, C. R. Phys. **7**, 6 (2006)
19. S.G. Ovchinnikov, Phys. Usp. **46**, 21 (2003)
20. A.V. Narlikar, *Magnetic Superconductors*, Studies of High Temperature Superconductors, vol. 46 (Nova Science, New York, 2003)
21. C. Noce, A. Vecchione, M. Cuoco, A. Romano (eds.), *Ruthenate and Rutheno-Cuprate Materials: Unconventional Superconductivity, Magnetism and Quantum Phase Transitions*, LNP, vol. 603 (Springer, Berlin, 2002)
22. L.T. Yang, J.K. Liang, Q.L. Liu, J. Luo, G.B. Song, F.S. Liu, X.M. Feng, G.H. Rao, J. Appl. Phys. **95**, 2004 (1942)
23. S.G. Hur, D.H. Park, S.-J. Hwang, S.J. Kim, J.H. Lee, S.Y. Lee, J. Phys. Chem. B **1009**, 21694 (2005)
24. T.W. Kim, I.-S. Yang, S.-J. Hwang, Bull. Korean Chem. Soc. **30**, 2559 (2009)
25. I. Felner, U. Asaf, S. Reich, Y. Tsabba, Physica C **311**, 163 (1999)
26. N.D. Zhigadlo, P. Odier, J.Ch. Marty, P. Bordet, A. Sulpice, Physica C **387**, 347 (2003)
27. P.W. Klamut, B. Dabrowski, S.M. Mini, M. Maxwell, J. Mais, I. Felner, U. Asaf, F. Ritter, A. Shengelaya, R. Khasanov, I.M. Savic, H. Keller, A. Wisniewski, R. Pizniak, I.M. Fita, C. Sulkowski, M. Matusiak, Physica C **387**, 33 (2003)
28. I. Matsubara, N. Kida, R. Funahashi, J. Phys., Condens. Matter **13**, 5645 (2001)
29. J.L. Tallon, J.W. Loram, G.V.M. Williams, C. Bernhard, Phys. Rev. B **61**, R6471 (2000)

30. X.H. Chen, Z. Sun, K.Q. Wang, S.Y. Li, Y.M. Xiong, M. Yu, L.Z. Cao, Phys. Rev. B **63**, 064506 (2001)
31. T.P. Papageorgiou, E. Casini, H.F. Braun, T. Herrmannsdoerfer, A.D. Bianchi, J. Wosnitza, Eur. Phys. J. B **52**, 383 (2006)
32. C.W. Chu, Y.Y. Xue, S. Tsui, J. Cmaidalka, A.K. Heilman, B. Lorenz, R.L. Meng, Physica C **335**, 231 (2000)
33. N.J. Nor Azah, S.A. Halim, R. Abd-Shukor, Supercond. Sci. Technol. **18**, 1365 (2005)
34. O.I. Lebedev, G. Van Tendeloo, G. Cristiani, H.-U. Habermeier, A.T. Matveev, Phys. Rev. B **71**, 134523 (2005)
35. M. Abatal, E. Chavira, C. Filippini, V. García-Vázquez, J.C. Pérez, H. Noël, J. Low Temp. Phys. **157**, 57 (2009)
36. www.llb.cea.fr/fullweb/fp2k/fp2k_links.htm
37. V. García-Vázquez, N. Pérez-Amaro, A. Canizo-Cabrera, B. Cumplido-Espínola, R. Martínez-Hernández, M.A. Abarca-Ramírez, Rev. Sci. Instrum. **72**, 3332 (2001)
38. R.D. Shannon, Acta Crystallogr. A, Found. Crystallogr. **32**, 751 (1976)